CERES Cloud Property Retrievals from Imagers on TRMM, Terra, and Aqua

Patrick Minnis*[a], David Young[a], Sunny Sun-Mack[b], Patrick W. Heck[c]
David R. Doelling[c], Qing Z. Trepte[b]

[a]Atmospheric Sciences, MS 420, NASA Langley Research Center, Hampton, VA USA 23681;
[b]SAIC, 1 Enterprise Parkway, Suite 300, Hampton, VA USA 23666
[c]AS&M, Inc., 1 Enterprise Parkway, Suite 300, Hampton, VA USA 23666

ABSTRACT

The micro- and macrophysical properties of clouds play a crucial role in Earth's radiation budget. The NASA Clouds and Earth's Radiant Energy System (CERES) is providing simultaneous measurements of the radiation and cloud fields on a global basis to improve the understanding and modeling of the interaction between clouds and radiation at the top of the atmosphere, at the surface, and within the atmosphere. Cloud properties derived for CERES from the Moderate Resolution Imaging Spectroradiometer (MODIS) on the *Terra* and *Aqua* satellites are compared to ensure consistency between the products to ensure the reliability of the retrievals from multiple platforms at different times of day. Comparisons of cloud fraction, height, optical depth, phase, effective particle size, and ice and liquid water paths from the two satellites show excellent consistency. Initial calibration comparisons are also very favorable. Differences between the *Aqua* and *Terra* results are generally due to diurnally dependent changes in the clouds. Additional algorithm refinement is needed over the polar regions for *Aqua* and at night over those same areas for *Terra*. The results should be extremely valuable for model validation and improvement and for improving our understanding of the relationship between clouds and the radiation budget.

keywords: radiation, clouds, remote sensing, cloud microphysics, climatology, MODIS, CERES, VIRS, Aqua, Terra

1. INTRODUCTION

Accurate retrievals of cloud micro- and macrophysical properties are necessary for improving both meso- and global scale models of weather and climate. Knowledge of those properties can provide the basis for understanding and quantifying the relationship between the Earth's radiation budget (ERB) and the water cycle. Since 1998, the Clouds and Earth's Radiant Energy System (CERES) project has been providing simultaneous retrievals of cloud properties and broadband radiative fluxes from instruments on several different satellites[1]. CERES is currently using three multispectral imagers, the Visible Infrared Scanner (VIRS) on the Tropical Rainfall Measuring Mission (*TRMM*) satellite and the Moderate Resolution Imaging Spectroradiometer (MODIS) on *Terra* and *Aqua*, to remotely sense a host of cloud properties on a global basis at different times of day coincident with the CERES broadband flux data. For the radiation budget and overall reliability, the cloud fields derived from the different satellites should be as consistent as possible in terms of the methodologies used in the retrievals and the absolute calibrations of the raw imager radiances. Except for time-space sampling differences, the results should be the same from a given imager. In a previous study[2], it was demonstrated that the CERES cloud property retrievals from *Terra* MODIS and *TRMM* VIRS were very consistent with most significant difference being the retrieval of smaller cloud droplet effective radii r_e from the *Terra* data. Preliminary comparisons of other parameters with climatological data also showed that the cloud amounts from both *TRMM* and *Terra* were in excellent agreement with the zonal means from long-term surface observations and were generally 0.07 - 0.08 less than those from the International Satellite Cloud Climatology Project (ISCCP) D2 dataset[3]. It

* p.minnis@nasa.gov; phone 1 757 864-5671; fax 1 757 864-7996; www-pm.larc.nasa.gov

Proceedings of SPIE Vol. 5235 Remote Sensing of Clouds and the Atmosphere VIII,
edited by Klaus P. Schäfer, Adolfo Comerón, Michel R. Carleer, Richard H. Picard
(SPIE, Bellingham, WA, 2004) · 0277-786X/04/$15 · doi: 10.1117/12.511210

was also reported that the CERES cloud optical depths *OD* were substantially larger than those from ISCCP. However, that earlier analysis[2] compared D2 log-averaged and CERES linear-averaged optical depths, a matchup that should have produced the relative differences that were reported. Comparisons with surface-based retrievals indicated that the mean CERES-derived cloud *OD* for stratus clouds were within 6% of their surface counterparts. Similar results were obtained for r_e. Except for difficulties with clouds at night over the polar regions, the initial study provided a high degree of confidence in the TRMM and Terra results. This paper continues the effort to ensure compatibility between the various CERES cloud products. Initial results from *Aqua* retrievals are presented and compared with the *Terra* results to determine the consistency of the cloud products and to examine some of the diurnally dependent features. These cloud properties have been already been responsible for dramatically improving the estimates of the ERB by facilitating the most accurate representation of the anisotropy of the radiance fields leaving the Earth-atmosphere system[4]. They will also be valuable for linking the hydrological cycle and ERB and for improving climate model processes.

2. DATA & METHODOLOGY

Aqua has a 1330 LT equatorial crossing and began producing MODIS imagery in early summer 2002. *Terra*, which started producing useable MODIS data in late winter of 2000, nominally crosses the Equator at 1030 LT. The *TRMM*, launched during late 1997, continues to provide coverage at all local hours between 37°N and 37°S over a 46-day period. VIRS data are used here only for evaluating the relative calibrations of the *Terra* and *Aqua* MODIS, , hereafter simply *Terra* and *Aqua*, channels. Every other 1-km MODIS pixel and scan line was skipped for CERES to achieve an effective 2-km resolution to minimize processing time and data storage. Results from CERES *Terra* Edition 1a and *Aqua* Beta 1 version are used here.

Each MODIS pixel is initially classified as clear or cloudy using updated versions of the CERES classification schemes[5-6] that rely on the radiances taken at 0.64 (visible), 1.6 or 2.1 (near infrared), 3.7 (solar infrared), 11 (infrared), and 12 (split window) μm. The 1.6-μm channel is used for the VIRS and *Terra* near-infrared data, but the 2.1-μm channel is used for *Aqua* because the *Aqua* 1.6-μm channel had several dead sensors. The radiances are compared with predicted clear-sky radiances based on empirical estimates of spectral clear-sky albedo[7-8] and on skin temperatures from the European Center for Medium-range Weather Forecasting (ECMWF) reanalyses adjusted using empirical estimates of spectral surface emissivity[9] and atmospheric absorption calculated with the ECMWF vertical profiles of temperature and humidity. Because of differences between the 1.6- and 2.1-μm reflectances for clear snow surfaces, it was necessary to make some adjustments to the cloud mask algorithms. The mean reflectances from *Terra* taken over clear snow scenes in the Arctic and Antarctic between January and July 2001 were computed as functions of solar zenith angle (SZA) and viewing zenith angle (VZA) for 1.6 and 2.1-μm. The variation of the mean reflectances with VZA are shown in Fig. 1. Both the 1.6 and 2.1-μm reflectances increase with VZA but the 1.6-μm reflectance exceeds its 2.1-μm counterpart. The ratio of the former to the latter varies from 0.43 to 0.45. The average value of the ratio is 0.438. For cloud detection with the *Aqua* data, the model values used to predict the 1.6-μm clear-sky reflectances are multiplied by this mean ratio and compared with the observed 2.13-μm reflectances.

Cloud temperature T_c, height z_c, thickness, phase, effective droplet radius r_e or effective ice crystal diameter D_e, optical depth $O\square$, and water path *WP* are derived from these same radiances using one of three methods. The visible infrared solar-infrared split-window technique (VISST), an updated version of the 3-channel daytime method[10], is used during daytime, defined as the time when the solar zenith angle *SZA* is less than 82°. At night, the solar-infrared infrared split-window technique (SIST) is used to determine all of the parameters. The SIST, an improved version of the 3-channel nighttime method[10], uses thermal infrared data only. Thus, its retrievals are valid only for optically thin clouds. For clouds with $\tau < 8$ at night, default values are used for all parameters except phase, T_c, and z_c. The third method[11], the solar-infrared infrared near-infrared technique (SINT) is only applied to MODIS data during the daytime for clouds over snow or ice backgrounds. For *Aqua*, the 2.13-μm channel replaces the 1.6-μm channel in the SINT. The determination of the background surface as snow or ice can either come from the scene classification for adjacent clear pixels or from the snow and ice maps used in the CERES data stream[7-8]. All of the methods compute ice and liquid water solutions that simultaneously determine T_c, $O\square$, and particle size by matching the observed radiances to emittance and reflectance parameterizations that account for atmospheric attenuation and surface reflectance and emission. The cloud reflectances and emittances are included in the parameterizations using updated lookup tables for each specific channel[12]. The phase is selected for each pixel based on the cloud temperatures, the availability of a solution, and the altitude of the cloud.

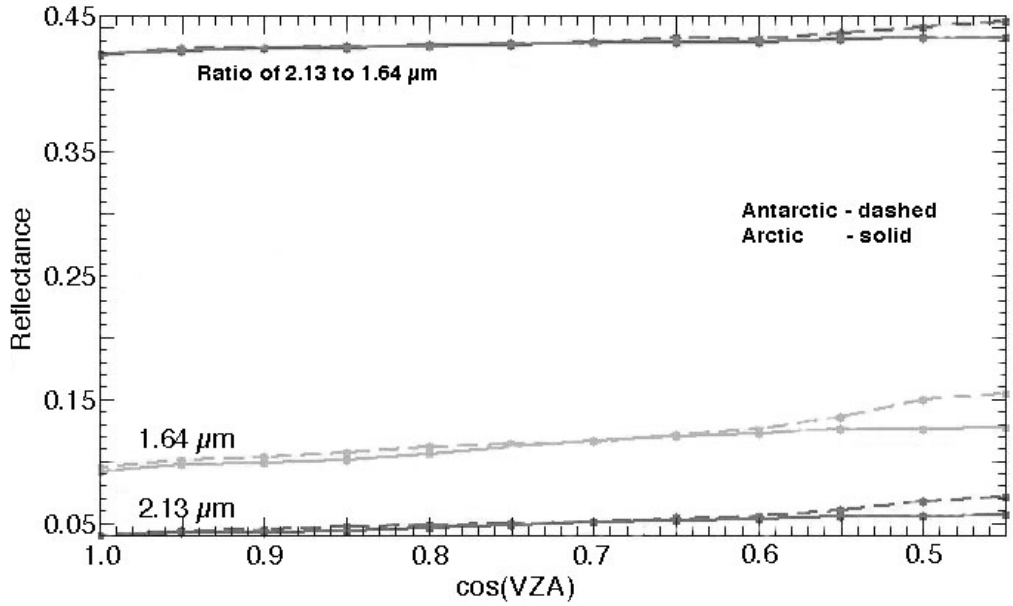

Figure 1. Mean near-infrared reflectances over random clear snow scenes, January - August 2001 from *Terra* MODIS.

The pixel-level data are convolved into the footprint (10-20 km) of each CERES radiance to provide the link between clouds and the radiation budget. These single-scanner footprint (SSF) products include the cloud fraction and mean associated properties for up to two cloud layers. Edition-2 VIRS cloud products, currently available for January 1998 - August 2001, will be processed as long as the VIRS data are available. The CERES fluxes are available on the VIRS SSFs only from January -August 1998 and during March 2000 because of the CERES scanner failed. As of this writing, the CERES Edition-1 *Terra* cloud properties have been completed for the period March 2000 through October 2002. Preliminary analysis of the *Aqua* data has been completed for September - October 2002 and January 2003.

3. CALIBRATION & VALIDATION

Consistency between satellite datasets first requires that any differences in calibration must be taken into account. The relationships between the common VIRS and *Terra* channels have already been analyzed using VIRS as the common thread[13-14]. A similar approach is taken here to determine the consistency between the relevant *Terra* and *Aqua* channels. All VIRS radiances over ocean surfaces meeting the prescribed coincidence criteria[13] were matched with overlapping *Aqua* and *Terra* radiances for every other month. The scatterplot for each channel was used to compute a linear regression line as shown, for example, in Fig. 2 for the visible channel data for January 2003. In this example, the regression line slopes are 1.031 and 1.034 for *Aqua* and *Terra*, respectively. The corresponding offsets are -2.05 and -1.52 $Wm^{-2}sr^{-1}\mu m^{-1}$. The differences between these coefficients, which are similar to those found earlier for *Terra* and VIRS[13], are not statistically significant indicating nearly ideal correspondence between the *Terra* and *Aqua* visible channels. From month to month, the slopes for the 0.65-µm channels typically vary between 1.01 and 1.05 for both satellites. In a similar fashion, the slope for the linear fits between the VIRS and *Terra* 1.6-µm channels varies between 1.18 and 1.23. No statistics are available for the *Aqua* 2.13-µm channel because it is not part of the VIRS package.

The mean slope and offset between the *Aqua* and VIRS for brightness temperatures from the 3.7-µm channels are 0.996 and 1.28 K resulting in differences of -0.8 and 0.1 K at 200 and 300 K, respectively. For the same period (November 2002 - March 2003), the corresponding slopes and offsets for *Terra* and VIRS are 0.984 and 5.41 K, respectively. The respective differences from the mean fit at 200 and 300 K are 2.1 and 0.5 K. Thus, the *Terra* 3.7-µm channel measures higher solar infrared temperatures than *Aqua* with mean differences ranging between 3 K and 0.4 K between 200 and 300 K. This difference would translate to somewhat larger retrieved cloud droplet sizes for *Aqua* compared to *Terra*. The infrared slope and offset for *Aqua* are 1.005 and-1.93 K, respectively, with differences of -0.8 and 0.3 K at 200 and

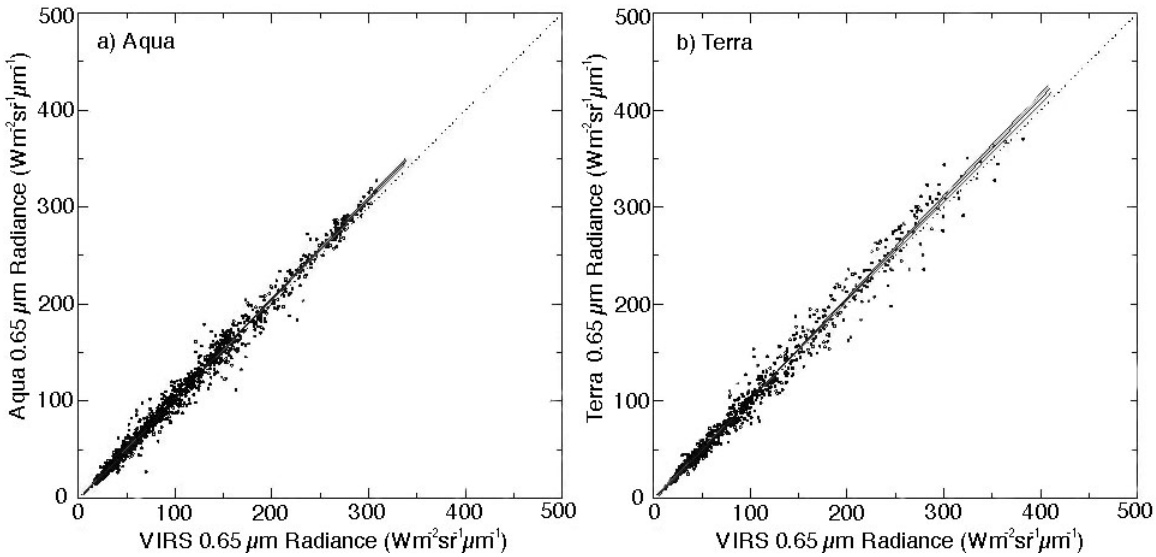

Figure 2: Scatterplots and linear regression fits for matched VIRS and (a) *Aqua* and (b) *Terra* MODIS data taken during March 2000.

300 K, respectively. The corresponding differences for the VIRS and *Terra* fits are -0.2 and 0.0 K for a slope of 1.002 and an offset of -0.61. For the split-window channels, *Terra* tends to measure slightly greater values at low temperatures with differences of 1.2 and 0.9 K at 200 and 300 K compared to -0.4 and 1.0 K for *Aqua* at the same VIRS temperatures. The mean slopes for the *Terra* and *Aqua* split-window channel fits with VIRS data are 0.997 and 1.014, respectively with corresponding offsets of 1.84 and -3.18 K. These preliminary calibration comparisons suggest that the *Terra* 12-µm channel runs about 0.8 K warmer than *Aqua*, on average. The mean difference for the 11-µm channels is less than 0.2 K.

A variety of methods are being used to verify the results including climatology, surface data, and other satellite observations as discussed earlier. Similar methods are being used for *Aqua*. The mean zonal cloud amounts from *Aqua* for September and October 2003 and from surface observations taken for the same months between 1971 and 1996[15] in Fig. 3 generally agree well in magnitude and distribution. One exception is in the Arctic, where during both months, the surface observations yield more cloud cover and all of the CERES observations are taken at night or in near-terminator conditions. Over the oceans south of 40°S, CERES detects more cloudiness. The surface climatology in those regions is based on very poor spatial sampling. These results highlight the difficulty of accurately detecting clouds in poorly lit

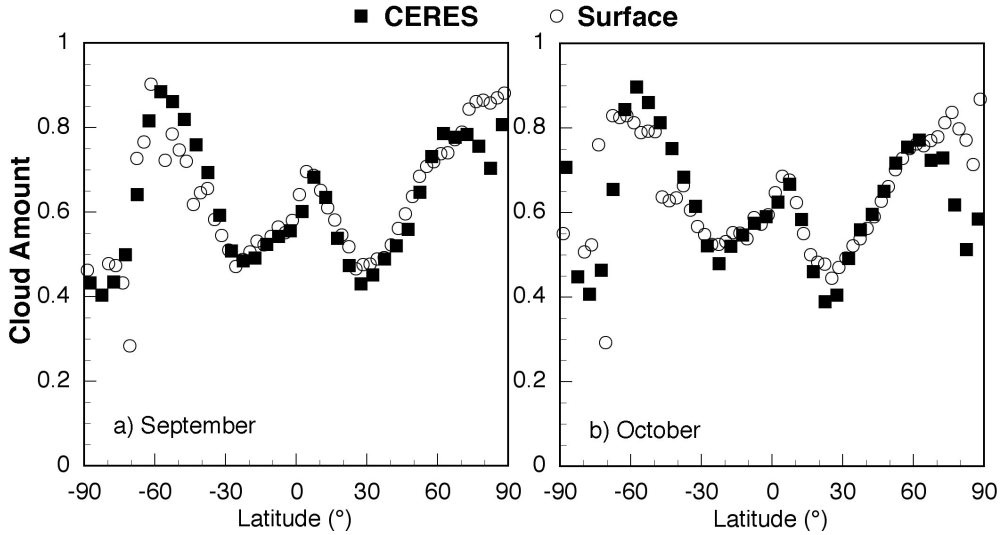

Figure 3: Monthly mean total cloud amounts from CERES *Aqua* (2003) and from surface observations (1971-1996).

conditions over snow and ice. Although comparisons of additional *Aqua* cloud parameters with other satellite and surface-based datasets are underway, these initial results demonstrate that the CERES *Aqua* cloud amounts are in line with previous datasets.

4. RESULTS AND CONSISTENCY

The mean October 2002 daytime cloud amounts *Ac* from *Aqua* and *Terra* are plotted in Fig. 4 along with the mean daytime effective cloud heights from *Aqua*. The general patterns in *Ac* are very similar for both satellites. The regions dominated by low-level marine stratocumulus clouds have less cloudiness at 1330 LT compared to that at 1030 LT. Over land and many areas with deep convection (indicated by $z_c > 8$ km), the cloud cover is greater at 1330 LT than during the midmorning. These variations are consistent with climatology. Closer examination of the cloud amounts reveals a slight discontinuity at 60°N. It is most apparent over northern Russia and the Norwegian Sea. This artifact is the result of switch from the standard cloud mask to the polar algorithm and will be eliminated in later versions of the analyses. Mean cloud heights under the marine subtropical high pressure systems and the Arctic Ocean are generally less than 2 km. Over the oceans surrounding Antarctica, z_c varies between 2 and 4 km, heights consistent with the predominance of stratus, altostratus, and nimbostratus in those areas[16]. Over the deserts of North Africa and southwestern Asia, the cloud amounts are slightly greater during the afternoon. From *Aqua*, those desert cloud amounts vary from less than 0.1 to nearly 0.4 in patterns consistent with those from surface observations[17]. Cloud heights over those deserts are generally around 8 km, on average, consistent with the predominance of the cirrus and altocumulus cloud types there[17].

The mean daytime water cloud optical depths for October 2002 from *Aqua* and *Terra* are plotted in Figs. 5a and 5b, respectively. The corresponding mean values of effective droplet radius from *Aqua* are shown in Fig. 5c. Mean *OD* appears to increase during the afternoon over the trade cumulus areas (green areas in the Tropics), the tropical convergence areas, the Amazon Basin, parts of central Africa, eastern China, and the eastern United States of America. It decreases over Russia, and the subtropical stratocumulus zones. A decrease in *OD* during the day is typical for subtropical marine stratus clouds[18]. Over the oceans surrounding Antarctica, the *Aqua* retrievals produce extremely large *OD*s, especially over regions with sea ice. The corresponding *Terra OD*s are generally between 8 and 16 as a result of applying the SINT retrieval with 1.6 μm replacing the visible channel. Apparently, in this beta version for *Aqua*, the SINT needs further adjustment for the differences between the 1.6 and 2.1-μm channels.

Mean cloud droplet sizes are obviously greater over ocean than over land as a rule. Larger droplets over land tend to occur in areas with extensive deep convection (e.g., central Africa or the Amazon Basin) or pristine areas such as the boreal forests or northern tundras. Areas with smaller droplets over water are generally limited to marine stratus regions and off the east coasts of the continents. The smallest oceanic cloud droplets are found around the coasts in the subtropical stratus areas. The values of r_e for *Terra* (not shown) follow the same patterns as those in Fig. 5c. However, they tend to be slightly smaller over most marine areas and differ little over land areas except for the convective regions where the *Aqua* values are larger. The only area over ocean where r_e obviously decreases during the day is off the coast of Chile where the area with $r_e < 10$ μm is greater for *Aqua*. Similar diurnal changes in effective droplet radius have been observed in earlier studies[19].

Cloud amounts from *Terra* and *Aqua* can be explored in more detail using Fig. 6, which shows the mean zonal values for land and ocean separately for daytime and nighttime. During daytime (Fig. 6a), *Ac*(*Aqua*) is generally smaller than *Ac*(*Terra*) over ocean, especially in the southern hemisphere. The exception is the intertropical convergence zone near 10°N. Over land, *Ac*(*Aqua*) > *Ac*(*Terra*), except over the polar regions where additional algorithm refinement is required. At night, *Ac*(*Aqua*) and *Ac*(*Terra*) are generally much closer than their daytime counterparts over both land and ocean. Nighttime differences between the two satellites are not as uniform in sign as during the day. The difficulty with cloud detection at night over the polar regions is quite evident in Figure 6b. Except for those polar areas, the differences between the *Aqua* and *Terra* cloud fractions are as expected. The distribution of ice and water clouds (Fig. 7) during the daytime tells a slightly different story than Fig. 6a. Liquid water clouds over ocean decrease during the afternoon at all latitudes while the coverage by ice clouds increases, especially over the Southern Ocean. The increase in ice clouds is consistent with a rise in overall cloudiness in the convergence areas. South of 45°S, the greater phase changes are most likely due to the algorithm differences between using the 1.6 and 2.13-μm channels in the phase determination process.

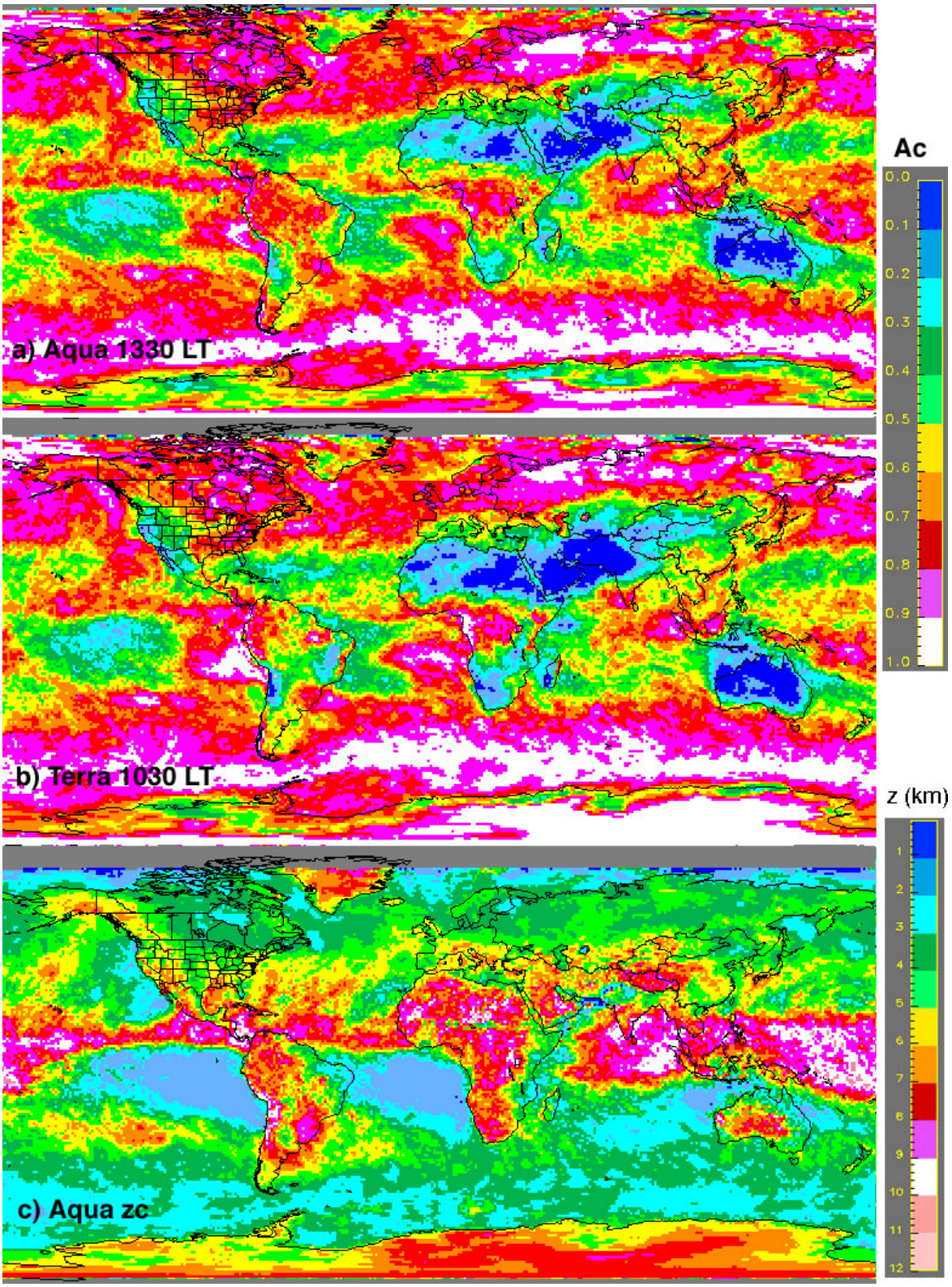

Figure 4: Mean daytime CERES cloud amounts from (a) *Aqua* and (b) *Terra*, and (c) cloud heights from *Aqua*, October 2002.

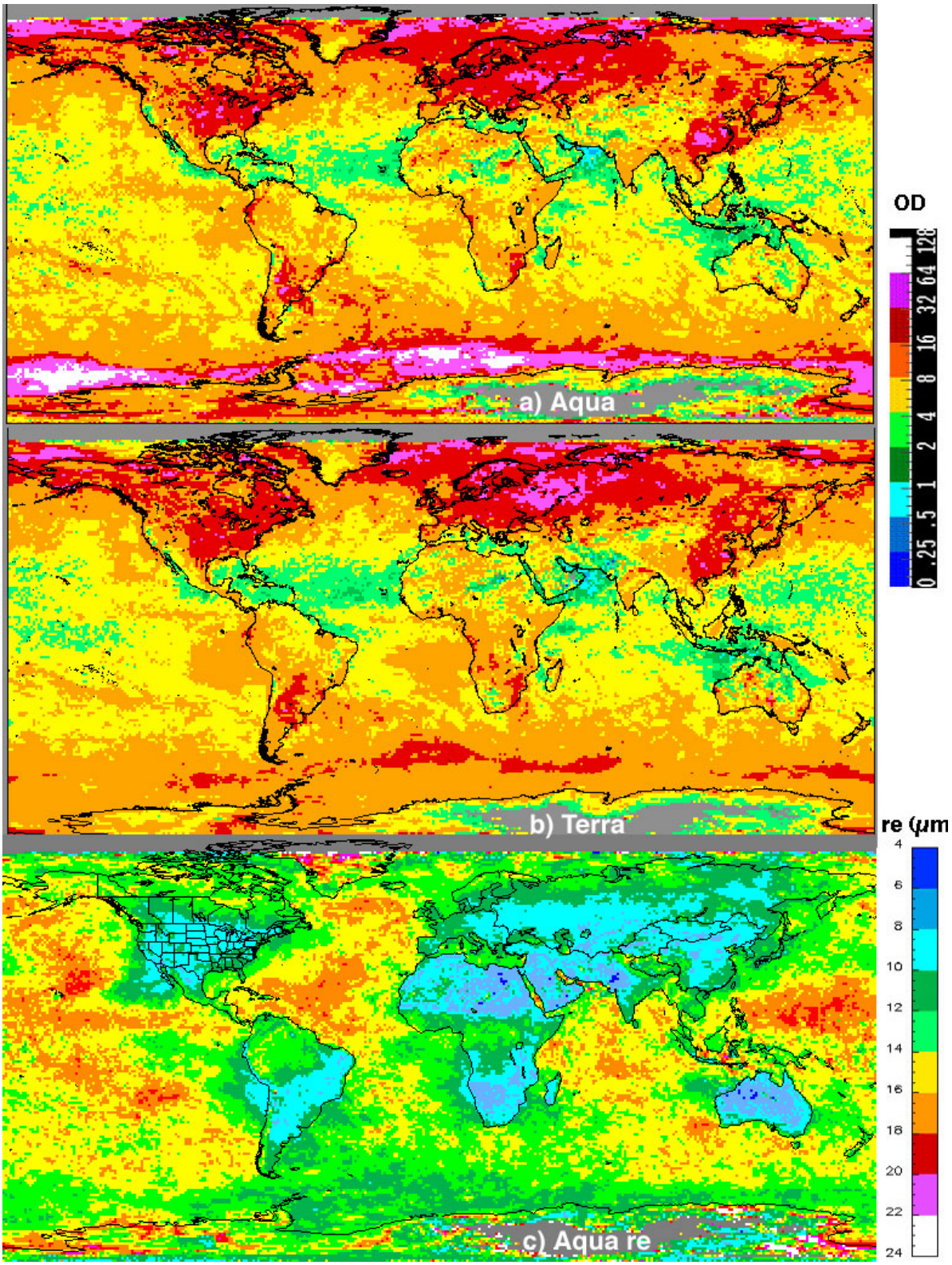

Figure 5: Mean daytime CERES cloud *OD* from (a) *Aqua* and (b) *Terra*, and (c) r_e from *Aqua*, October 2002.

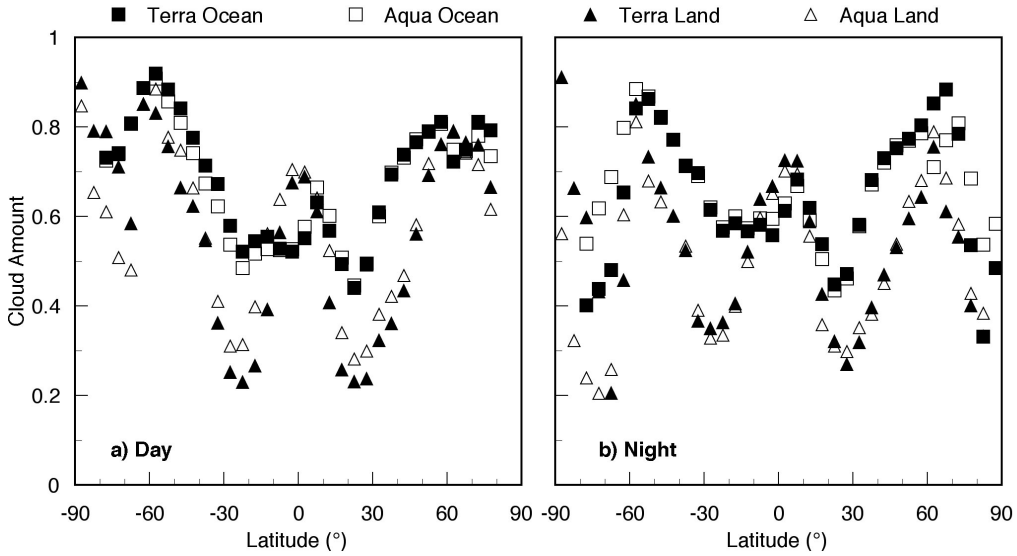

Figure 6: Comparisons of *Terra* and *Aqua* mean zonal cloud amounts, October 2002.

Over tropical land areas, ice cloud cover (Fig. 7d) increases during the afternoon at the expense of water clouds (Fig. 7b) in some zones. In the subtropics, both ice and water cloud amounts increase by a small amount. Over polar land areas, *Terra* classifies more clouds as ice than *Aqua*, perhaps as a result of the channel differences.

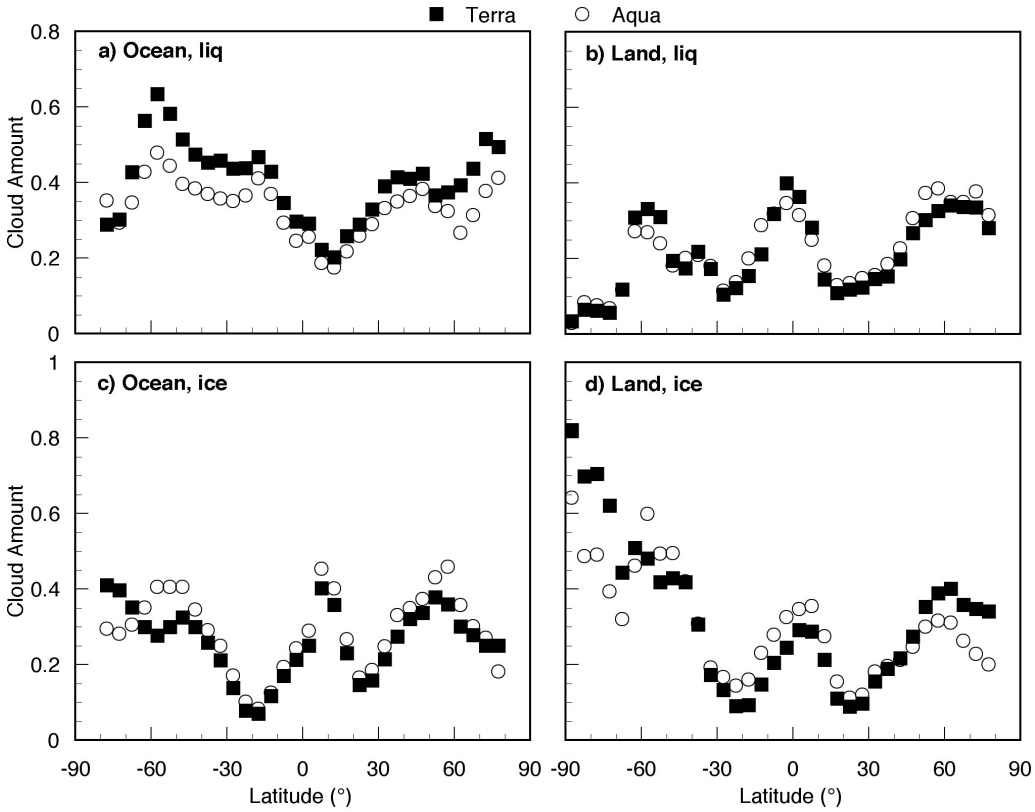

Figure 7: Mean zonal daytime cloud amounts by phase from *Terra* and *Aqua*, October 2002.

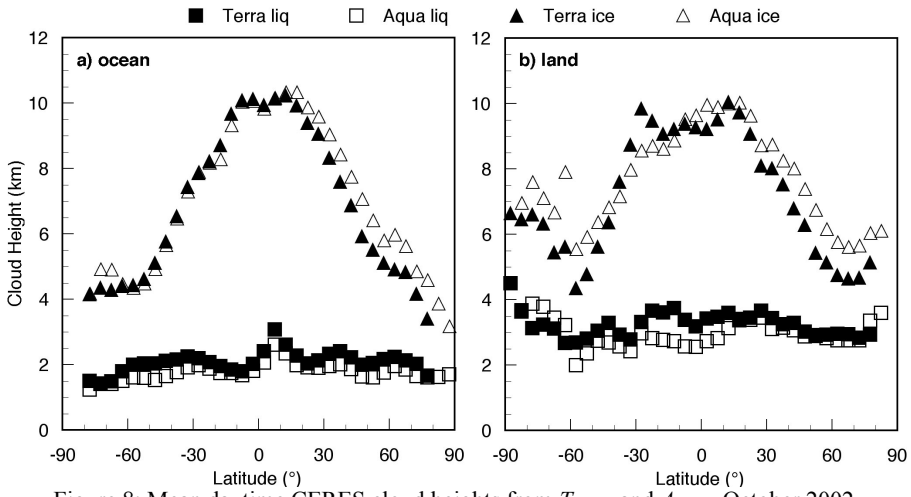

Figure 8: Mean daytime CERES cloud heights from *Terra* and *Aqua*, October 2002.

Water cloud heights over ocean and land are almost uniformly less during the afternoon than during the midmorning period (Fig. 8). In non-polar regions (equatorward of 60°), water clouds from *Aqua* are, on average, 300 and 430-m less than those from *Terra* over ocean and land, respectively. This *Aqua-Terra* discrepancy cannot be explained by calibration differences given the results for the 11-µm channels noted earlier. Part of the difference over ocean can be attributed to the diurnal cycle in stratus and stratocumulus, which tend to decrease in height as they break up. Stratus clouds tend to peak during the morning over land also, but the total cloud cover usually peaks around noon[17]. The differences over land may be the result of more altostratus during the morning and/or stratus clouds that are higher than cumulus, of differences in the morning and afternoon temperature profiles, or of greater impact of the background temperature on height during the afternoon when scattered cumulus clouds are prevalent. This difference will require further exploration. The ice cloud heights are greater in Northern Hemisphere over both land and ocean during the afternoon with minimal differences over the Southern Hemisphere. On average for non-polar regions, the ice clouds are 200 and 350-m higher at 1330 LT than at 1030 LT over ocean and land, respectively.

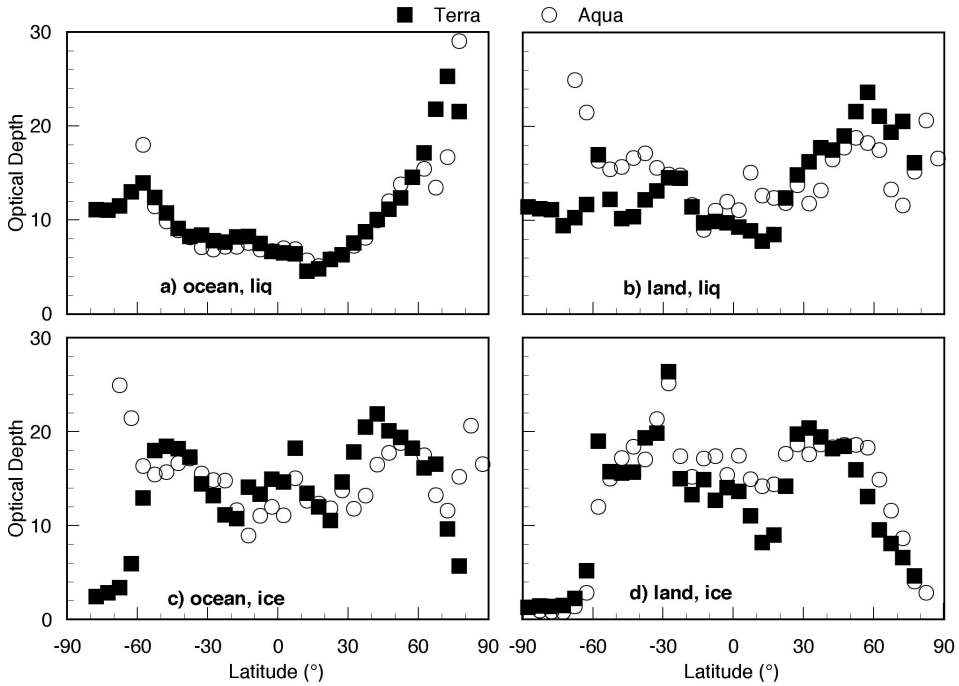

Figure 9: Same as Figure 8, except for optical depths.

Maritime water cloud *OD*s from *Aqua* and *Terra* (Fig. 9a) are very similar despite the regional differences seen in Fig. 5. The mean difference is 0.0 for non-polar areas. Over non-polar land (Fig. 9b), the mean *OD*s are greater by 0.9 during the morning, perhaps due to the diurnal differences in stratus and cumulus coverage. The average *OD*s of ice clouds are 1.5 greater during the morning over non-polar ocean compared to being 1.4 less over land. These land-ocean differences are probably due to differences in the timing of the most intense convective events. The differences in the polar regions highlight the need for refinement of the SINT using the 2.13-µm channel on *Aqua*.

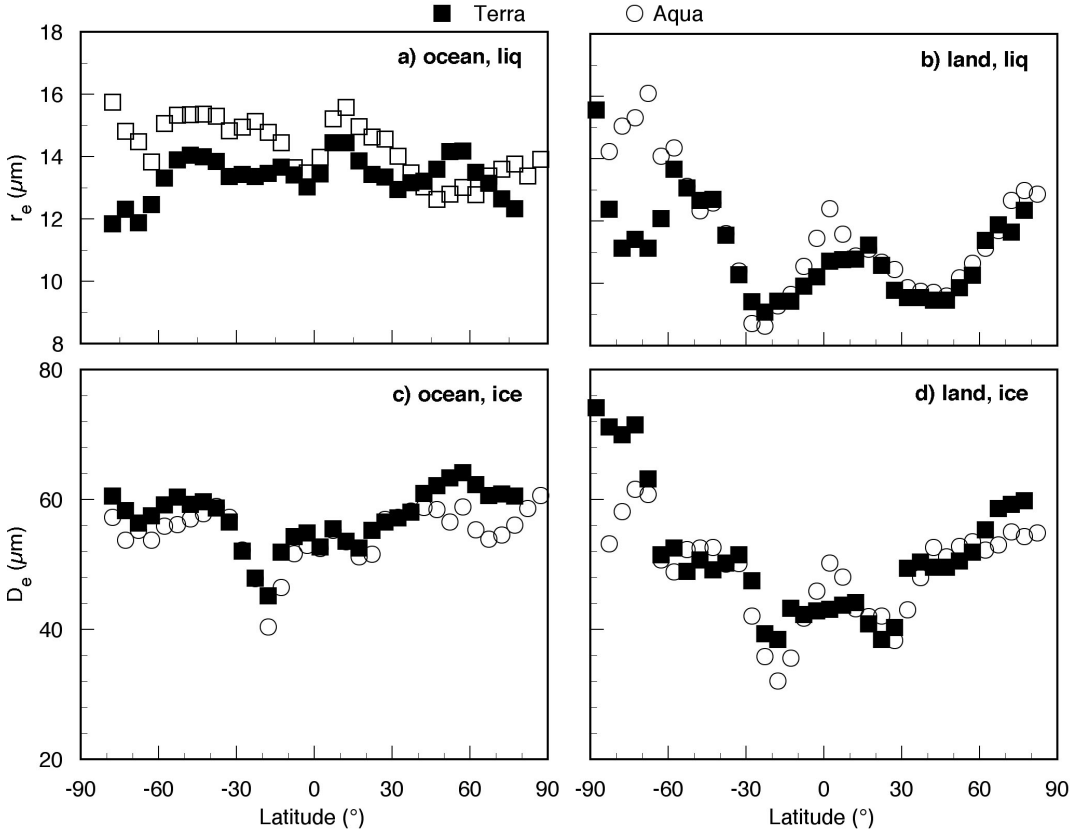

Figure 10: Same as Figure 8, except for effective cloud particle size.

As noted for Fig. 5, the mean cloud droplet sizes from *Aqua* generally exceed those from *Terra*. This finding is reinforced with a comparison of the zonal mean cloud particle sizes in Fig. 10. The greatest differences are evident in the Southern Hemisphere over water (Fig. 10a). The mean r_e from *Aqua* is greater than its *Terra* counterpart only over the northern midlatitude oceans. For non-polar regions, the mean difference is 0.8 µm. This tendency is not as obvious over land (Fig. 10b), where the most significant difference occurs in the tropical convergence areas and over Antarctica. The mean non-polar difference is only 0.2 µm. The apparent 3.7-µm calibration differences mentioned earlier could result in a retrieval bias of as much as 0.5 µm. Thus, the afternoon values of r_e may actually be smaller than during the morning over land. Over ocean, the mean effective diameter D_e of the ice crystals (Fig. 10c) for non-polar regions is 54.3 µm, a value that is 2.0-µm less than the *Terra* mean. None of the *Aqua* zonal D_e means exceeds any from *Terra*. Over land (Fig. 10d), the differences between the *Terra* and *Aqua* values of D_e vary from positive to negative. On average, D_e(*Aqua*) is only 0.2-µm greater than D_e(*Terra*). Discrepancies between the *Terra* and *Aqua* cloud particle sizes are most dramatic over ice and snow-covered areas providing further impetus for refining the polar masks and retrieval algorithms. The *OD*s and particle sizes are used to compute both liquid and ice water paths, *LWP* and *IWP*, respectively. For non-polar regions, *LWP*(*Aqua*) exceeds *LWP*(*Terra*) by 4.6 gm^{-2} in the mean over ocean compared to only 0.4 gm^{-2} over land. The 37.2 gm^{-2} deficit in *IWP*(*Aqua*) relative to *IWP*(*Terra*) over ocean is compensated by an *Aqua IWP* surplus of 38.0 gm^{-2} over land during October 2002.

5. CONCLUDING REMARKS

A robust methodology has been developed for retrieving cloud properties from high-resolution imager data during day and night. It has been applied to imager data from 3 different satellites. The consistency between the VIRS Edition 2 and *Terra* MODIS Edition 1 retrievals[2,20] is complemented by the even greater compatibility between *Terra* Edition 1a and *Aqua* Version Beta 1 demonstrated here. The current results should be immediately valuable for examining spatial and temporal variations of cloud properties in non-polar regions. Studies of clouds over ice and snow-covered regions during the daytime should be possible with the current *Terra* Edition 1a data. Future releases of the CERES data, including non-beta *Aqua* products, will be based on improved polar algorithms that should minimize discontinuities in the cloud mask, uncertainties in nocturnal polar retrievals, and discrepancies in the derived cloud properties. In addition to serving as valuable data for radiation budget analyses, the CERES cloud datasets should also be useful for validating and improving general circulation models and cloud process parameterizations. The CERES cloud and radiation products are available to the general public at http://eosweb.larc.nasa.gov/HBDOCS/langley_web_tool.html.

ACKNOWLEDGMENTS

This research is sponsored by the NASA Earth Enterprise System through the CERES Program.

REFERENCES

1. Wielicki, B. A., et al., 1998, Clouds and the Earth's Radiant Energy System (CERES): Algorithm overview. *IEEE Trans. Geosci. Remote Sens.*, **36**, 1127-1141.
2. Minnis, P., D. F. Young, B. A. Weilicki, S. Sun-Mack, Q. Z. Trepte, Y. Chen, P. W. Heck, and X. Dong, A global cloud database from VIRS and MODIS for CERES. *Proc. SPIE 3rd Intl. Asia-Pacific Environ. Remote Sensing Symp. 2002: Remote Sens. of Atmosphere, Ocean, Environment, and Space*, Hangzhou, China, October 23-27, 2002.
3. Rossow, W. B. and R. A. Schiffer, Advances in understanding clouds from ISCCP. *Bull Am. Meteor. Soc.*, **80**, 2261-2287, 1999.
4. Loeb, N. G. et al., Angular distribution models for top-of-atmosphere radiative flux estimation from the Clouds and the Earth's Radiant Energy System instrument on the Tropical Rainfall Measuring Mission satellite. Part I: Methodology. In press, *J. Appl. Meteorol.*, 2002.
5. Trepte, Q., Y. Chen, S. Sun-Mack, P. Minnis, D. F. Young, B. A. Baum, and P. W. Heck, Scene identification for the CERES cloud analysis subsystem. *Proc. AMS 10th Conf. Atmos. Rad.*, Madison, WI, June 28 – July 2, 169-172, 1999.
6. Trepte, Q. Z., P. Minnis, and R. F. Arduini, Daytime and nighttime polar cloud and snow identification using MODIS. *Proc. SPIE Conf. Optical Remote Sens. of Atmosphere and Clouds III*, Hangzhou, China, Oct. 23-27, 2002.
7. Sun-Mack, S., Y. Chen, T. D. Murray, P. Minnis, and D. F. Young, Visible clear-sky and near-infrared surface albedos derived from VIRS for CERES. *Proc. AMS 10th Conf. Atmos. Rad.*, Madison, WI, June 28–July 2, 422-425, 1999.
8. Chen, Y., S. Sun-Mack, Q. Z. Trepte, P. Minnis, and D. F. Young, Solar zenith angle variation of clear-sky narrowband albedos derived from VIRS and MODIS. *Proc. 11th AMS Conf. Atmos. Rad.*, Ogden, UT, June 3-7, 152-155, 2002.
9. Chen, Y., S. Sun-Mack, Surface spectral emissivity derived from MODIS data. *Proc. SPIE Conf. Optical Remote Sens. of Atmosphere and Clouds III*, Hangzhou, China, Oct. 23-27, 2002.
10. Minnis, P. et al., Cloud Optical Property Retrieval (Subsystem 4.3). In *Clouds and the Earth's Radiant Energy System (CERES) Algorithm Theoretical Basis Document, Volume III: Cloud Analyses and Radiance Inversions (Subsystem 4)*, *NASA RP 1376 Vol. 3*, edited by CERES Science Team, pp. 135-176, 1995.
11. Platnick, S., J. Y. Li, M. D. King, H. Gerber, and P. V. Hobbs, A solar reflectance method for retrieving cloud optical thickness and droplet size over snow and ice surfaces. *J. Geophys. Res.*, **106**, 15185-15199, 2001.
12. Minnis, P., D. P. Garber, D. F. Young, R. F. Arduini and Y. Takano, Parameterizations of reflectance and effective emittance for satellite remote sensing of cloud properties. *J. Atmos. Sci.*, **55**, 3313–3339, 1998.

13. Minnis, P., L. Nguyen, D. R. Doelling, D. F. Young, W. F. Miller, and D. P. Kratz, Rapid calibration of operational and research meteorological satellite imagers, Evaluation of research satellite visible channels as references. *J. Atmos. Oceanic Technol.*, **19**, 1233-1249, 2002.
14. Minnis, P., L. Nguyen, D. R. Doelling, D. F. Young, W. F. Miller, and D. P. Kratz, Rapid calibration of operational and research meteorological satellite imagers, Part II: Comparison of infrared channels. *J. Atmos. Oceanic Technol.*, **19**, 1250-1266, 2002.
15. Hahn, C. J., and S. G. Warren, *Extended Edited Synoptic Cloud Reports from Ships and Land Stations Over the Globe, 1952-1996.* NDP026C, Carbon Dioxide Information Analysis Center, Oak Ridge National Laboratory, Oak Ridge, TN, 1999.
16. Warren, S.G., C.J. Hahn, J. London, R.M. Chervin, and R.L. Jenne, Global distribution of total cloud cover and cloud type amounts over ocean, NCAR Tech. Note NCAR/TN-317+STR, 212 pp., 1988.
17. Warren, S.G., C.J. Hahn, J. London, R.M. Chervin, and R.L. Jenne, Global distribution of total cloud cover and cloud type amounts over land, NCAR Tech. Note NCAR/TN-273+STR, 229 pp., 1986.
18. Ayers, J. K., P. W. Heck, A. D. Rapp, P. Minnis, D. F. Young, W. L. Smith, Jr., and L. Nguyen, A one-year climatology of cloud properties derived from GOES-8 over the southeastern Pacific for PACS. *Proc. 11th AMS Conf. Cloud Physics.*, Ogden, UT, June 3-7, CD-ROM, P2.10, 2002.
19. Han, Q-Y., W. B. Rossow and A. A. Lacis, Near-global survey of effective cloud droplet radii in liquid water clouds using ISCCP data. *J. Climate,* **7**, 465-497, 1994.
20. Minnis, P., et al., Seasonal and diurnal variations of cloud properties derived for CERES from VIRS and MODIS data. *Proc. 11th AMS Conf. Atmos. Rad.*, Ogden, UT, June 3-7, 20-23, 2002.